Journal of King Saud University – Science 34 (2022) 101872

Contents lists available at ScienceDirect

Journal of King Saud University – Science

journal homepage: www.sciencedirect.com

Original article

Bis-(*N*-aminoethylethanolamine)-Copper(II) nanocatalysis (AEEA-Cu(II)-NPs) meditated to synthesis a series of 2-thioxo-1,2,3,4-tetrahydropyrimidine-5-carboxamide derivatives: Characterization of theoretical, computational and evaluation of molecular docking, and cytotoxicity activities

Chidambaram SathishKumar [a], Radhakrishnan Surendrakumar [a], Gurusamy Raman [b], Daoud Ali [c], Saud Alarifi [c], Akbar Idhayadhulla [a,*]

[a] Research Department of Chemistry, Nehru Memorial College (Affiliated to Bharathidasan University), Puthanampatti 621007, Tiruchirappalli District, Tamil Nadu, South India
[b] Department of Life Science, Yeungnam University, Gyeongsan, Gyeongbuk-do 38541, South Korea
[c] Department of Zoology, College of Sciences, King Saud University (KSU), P.O. Box 2455, Riyadh 11451, Saudi Arabia

ARTICLE INFO

Article history:
Received 6 September 2021
Revised 23 January 2022
Accepted 24 January 2022
Available online 5 February 2022

Keywords:
Biginelli reaction
2-Thioxo-pyrimidine-5-carboxamide
Copper nanoparticles
HOMO
LUMO

ABSTRACT

In this work, bis-(*N*-aminoethylethanolamine)-Copper (II) nano (**AEEA-Cu(II)-NPs**) catalysis was synthesized and used as a catalyst in Biginelli reactions. Synthesized nanocatalysis was characterized by UV, FT-IR, XRD, SEM, and particle size distribution analysis. The title compounds of thioxo-1,2,3,4-tetrahydropyrimidine-5-carboxamide derivatives (**1a-1o**) were synthesized via Biginelli method, the reaction was carry out via **AEEA-Cu(II)-NPs** catalysis. Synthesized compounds (**1a-1o**) were characterized by FT-IR, ^{1}H NMR, ^{13}C NMR, mass spectrometry, and elemental analysis. The spectral data of compound **1a** was confirmed by the comparison of both experimental and theoretical values. GC-EI-MS analysis of the characteristic protonation pathways for GC-EI-MS fragmentation of synthetic 2-thioxo-pyrimidine-5-carboxamide derivatives is reported. Computing methods of compound **1a** was studied such as optimize the geometry, frontier molecular orbital analysis (HOMO-LUMO), and molecular electrostatic potential (MESP). In cytotoxicity screening, compounds were tested against. Cell lines 2HepG2 (liver), MCF-7 (breast), and HeLa (cervical) cancer cell lines. Molecular docking was used to determine the inter and intramolecular interactions. In order to determine the most effective pyrimidine derivatives (1f and 1 g) for the protein 4FM9, and Autodock Vina 1.1.2 software was used in conjunction with the binding mode of **fluorouracil** as a reference compound. The compounds **1f** and **1g** were extremely effective against HepG2 cells compared to fluorouracil. During docking studies, **1f** showed a higher attraction for the 4FM9 protein (−6.5 kcal/-mol) than fluorouracil (−5.4 kcal/mol). The compounds **1f,** and **1g** showed impressive inhibitory properties in cytotoxic screening as compared to the reference compound. Due to the docking studies and cytotoxicity screening results, the new compounds look promising as therapeutic agents.

1. Introduction

In medicinal chemistry, heterocyclic rings have played a central role in the development of numerous important therapeutic agents. Pyrimidines (“m-Diazine”) have been considered breakdown products of uric acid since the beginning of organic chemistry. Alloxan was the first pyrimidine derivative to be synthesized by Brugnatelli by oxidizing uronic acid with nitric acid in 1818 (Lagoja, 2005). Pyrimidines (mainly uracil, thymine, and cytosine), this molecule has been isolated by hydrolysis of nucleic

* Corresponding author.
E-mail address: idhayadhulla@nmc.ac.in (A. Idhayadhulla).
Peer review under responsibility of King Saud University.

Production and hosting by Elsevier

https://doi.org/10.1016/j.jksus.2022.101872
1018-3647/

acids. All living things consist of nucleic acids, which are essential components of cells. Deoxyribonucleic acid (DNA) and ribonucleic acid (RNA) both contain cytosine, but uracil and thymine are found only in RNA and DNA, respectively (Agarwal, 2006). Pyrimidine skeletons can be found in other natural products, such as vitamin B1 (thiamine), as well as many synthetics, including barbituric acid and veranal, both hypnotics (Porter, 1979). It possess antioxidant (Abu-Hashem et al., 2011), antifungal (Basavaraja et al., 2005), antiviral (Storer et al., 2005), antihistaminic (Rahaman et al., 2009), antidiabetic (Lee et al., 2005), antibacterial (Holzol et al., 2006), anti-inflammatory (Sondhi et al., 2008), antileishmanial (Ram et al., 1992), herbicidal (Nezu et al., 1996), antihypertensive (Rana et al., 2004), antiallerggic (Juby et al., 1979), anticancer activities (Xie et al., 2009), anticonvulsant (Gupta et al., 1994), analgesic (Vega et al., 1990), and several pyrimidine compounds have exhibited antinociceptive effects in the central nervous system (CNS) (Rodrigues et al., 2005) and are also calcium channel blockers (Kumar et al., 2002). Examples of such compounds are emivirine (Fig. 1) and 5-ethyl-2-thioxo-2,3-dihydro-1*H*-pyrano[2,3-d] pyrimidinepyrano [2,3-d] pyrimidine-4,7-dione (Huang et al., 2012), methylthiouracil is used as a antithyroid agent and also a thioamide, closely related to propylthiouracil. In the pharmaceutical industry, 3,4-dihydropyrimidin-2(1*H*)-ones, which function as calcium channel blockers, antihypertensive drugs, and alpha-1-antagonists, are produced by the Biginelli reaction. The recent development of 3,4-dihydropyrimidin-2-(1*H*)-ones and their analogous drugs has greatly increased the production of antiviral, antibacterial, antitumor, and antihypertensive drugs. Described by Biginelli in 1893, the classical method for synthesis of 3,4-dihydropyridine-1-(1*H*)-ones is difficult to carry out, while yields are low. Researchers are learning about some new catalysts that will enhance the yield of the biginelli reaction, including $MgBr_2$, $KHSO_4$, NH_4Cl, $InBr_3$, and $FeCl_3{\cdot}6H_2O$, as well as some unconventional approaches, such as microwaves (Suresh and Sandhu, 2012). The reactions required by these protocols can be quite expensive, require acidic conditions, and take a long time to complete, or yield unsatisfactory results. For the Biginelli reaction, we will need to perform further research so that an effective catalyst can be designed. The Biginelli reaction was improved in 1987 by Atwal (Atwal et al., 1987). First enzyme-catalysed Biginelli synthesis using yeast protocol was reported by Kumar and Maurya (2007). Basically pyrimidinones are exhibiting a range of biological effects, including: antihypertensive (Alam et al., 2010), antiepileptic (Lewis et al., 2010), antimalarial (Chiang et al., 2009), anti-inflammatory (Mokale et al., 2010), antitubercular (Trivedi et al., 2010) and antioxidative (Ismaili et al., 2008). It is necessary to discover a new and inexpensive catalyst capable of making 3,4-dihydropyrimidine-2-(1*H*)-ones in neutral and mild conditions. Solvent-free organic reactions employ reagents without the use of a solvent, and are rapidly developing. Organic synthesis presents a challenging area for developing new strategies for synthesis of complex molecules. Under anhydrous conditions, many organic reactions take place using volatile organic solvents such as benzene, which are potentially carcinogenic and harmful to the environment. A safe, practical, and eco-friendly process is therefore needed. It is possible to achieve high yields of many exothermic reactions using the "Grindstone Chemistry" technique. Grinding initiates reactions, with friction transferring a small amount of energy. As part of this approach, catalysts are included such as $CeCl_3{\cdot}7H_2O$, $FeCl_3$-HCl, $ZnCl_2$, $CoCl_2$, $CuCl_2{\cdot}2H_2O$ etc. In the Biginelli reaction, we concentrated on the catalytic behaviour of the Cu(II) and ammonium compounds, that is bis(phenyl ammonium) tetrachloride cuprate (II), $(PhNH_3)_2CuCl_4$. Dihydropyrimidinones can be synthesized efficiently with Lewis acids, such as $Cu(OTf)_2$ (Pasunooti et al., 2011), $CuCl_2$, $Cu(NO_3)_2{\cdot}3H_2O$ (Wang et al., 2011), $Cu(NTf)_2$, [[Gmim]Cl–Cu(II)], Cu nanoparticles (Dewan et al., 2012), $Cu(acac)_2$[bmim]BF_4, poly(4-vinylpyridine-co-divinyl benzene)–Cu(II) complex (Yarapathi et al., 2004), and CuI. According to the above observation, we use Cu(II) nanocatalysis for synthesis of 2-thioxo-pyrimidine-5-carboxamide which conforms to a computational chemistry analysis and also shows cytotoxic effects.

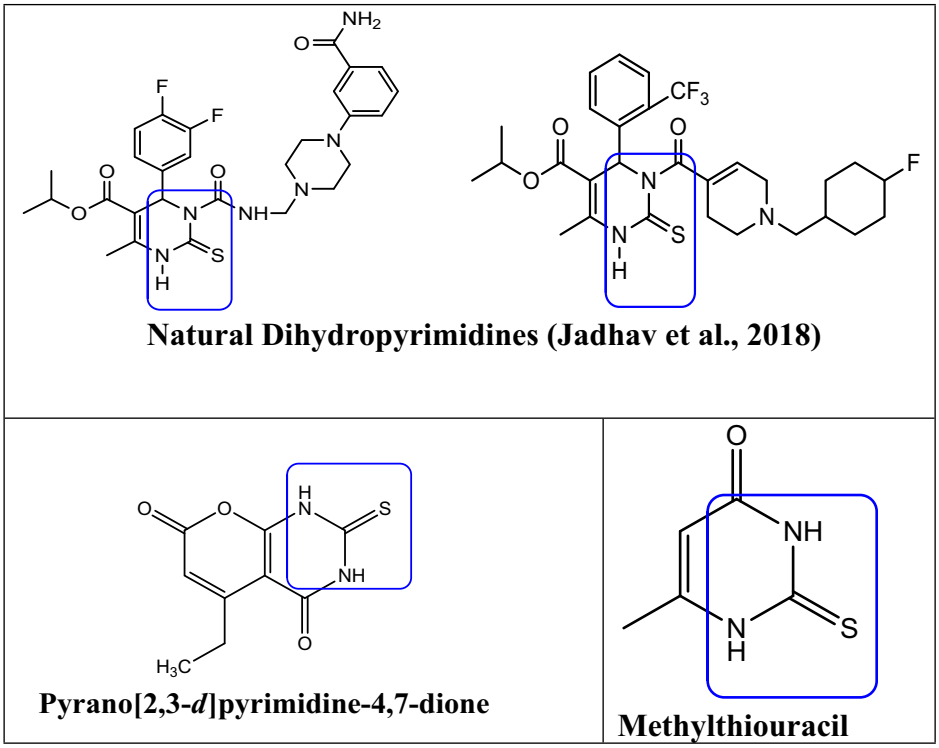

Fig. 1. Natural bioactive 2-thioxo pyrimidine.

2. Materiel and methods

2.1. Chemistry

2.1.1. AEEP-Cu(II)-Nps Copper nanoparticles synthesis

To create the mixture, $CuCl_2$ (0.5 mmol) and *N*-amino ethylethanolamine (1 mmol) in ethanol were added at room temperature to a mortar (Grindstone method) and ground for 15 min. The obtained solid mixed with 1 M NaOH (pH = 7). The prepared substance was dried and cleaned with suitable solvents after the reaction. Final product was obtained blue colure in nature.

2.1.2. Synthesis of 6-methyl-4-phenyl-2-thioxo-1,2,3,4-tetrahydropyrimidine-5-carboxylic acid hydrazide (1a)

In a 5-minute grinding operation, benzaldehyde (1 mmol), ethylacetoacetate (1 mmol), thiourea (1 mmol), substituted amine (1 mmol) and AEEA-Cu(II)-Nps were combined. The reaction was monitored using TLC. A solid mass is washed in cold water. The catalyst was soluble in water and decanted. The insoluble solid was filtered, dried, and then recrystallized in hot alcohol overnight before being acquired as pure product. For the remaining compounds, the same synthetic protocol was followed (**1b-1o**) (See Supporting Info for spectral characterization).

2.1.3. GC-EI-MS instrumentation

Single quadrupole GC-EI-MS perkin Elmer GCMS model GC clarus 680 and MS SQ8T (EI) with used Elite-5 (5% diphenyl/95% dimethyl polysiloxane) capillary columns −30 m × 0.25 mm × 0.25 μm (See Supporting Info for spectral characterization).

2.1.4. Computational methods

An ab initio CBS-QB3 model was used to elevate geometry and calculate frequency using the hybrid density functional theory (DFT) of Becke's three-parameter (B3) exchange-Lee, Yang, and Parr (LYP) correlation functional (B3LYP) in conjunction with the 6-311G(d,p) basis set and CCSD(T) follows to get limit of basis sets. Experimental details available in Supporting Info

2.1.5. Cytotoxic activity

On the basis of previous literature, cytotoxic properties of the newly synthesized compounds (**1a-1o**) were analysed (Surendra Kumar et al., 2011, 2017). Experimental details available in Supporting Info

2.1.6. Studies of molecular docking

Autodock vina 1.1.2 was used to study the interaction, binding mode between compounds **1f, 1g, fluorouracil** and the protein 4FM9 (Trott and Olson, 2010). Experimental details available in supporting information.

2.1.7. Prediction of ADME and molecular properties

Using Lipinski's "Rule of Five", the ADME and toxicity of compounds **1f**, **1g**, and **fluorouracil** were determined (Lipinski et al., 2001). Swiss ADME (Swiss ADME, 2021) predicted Lipinski's parameters. The assessment was conducted by calculating the tPSA (topological polar surface area) (Ertl et al., 2000). Absorption from the digestive tract is responsible for bioavailability (Daina and Zoete, 2016).

The percentage of calculation: % ABS = 109 − (0.345 × TPSA).

3. Result and discussion

3.1. Chemistry

3.1.1. Nanoparticle synthesis

Synthesis of bis-(*N*-amino ethylethanolamine)-Copper(II) nanoparticles (**AEEA-Cu(II)-NPs**) was prepared from grindstone stone method, reaction outline is represented in scheme 1. The $CuCl_2{\cdot}2H_2O$ (0.5 mmol) was grind with 15 min with using ligand of 2-((2-aminoethyl) amino) ethanol (1 mmol) by grindstone stone method at room temperature. The final product was formed blue precipitate, it was soluble in water. The fine compound was purified by using suitable solvent via re-precipitated method. Finally, obtained solid materials were characterized by FTIR, UV, SEM, XRD and particle size analysis for confirmation of nanoparticle formation.

3.1.2. UV–Visible studies

Cu nano particles were formed from interaction of AEEA ligand to from Cu-NPs. The Cu-NPs absorption was recorded at 556 nm whereas AEEA ligand shows no peak obtained between in 500–700 nm. The UV-visible spectrum is showing in Fig. 2. **AEEA**-Cu(II)-NPs exhibited the absorption bands at 556 nm.

3.1.3. FT-IR studies

Fig. 7 (Available in supporting information) shows vibrations frequency of AEEA-Cu(II)-NPs. In order to analyze the presence of vibrational frequency in the compounds, IR values were compared to the literature. The O − H stretching in centre of Cu, which was

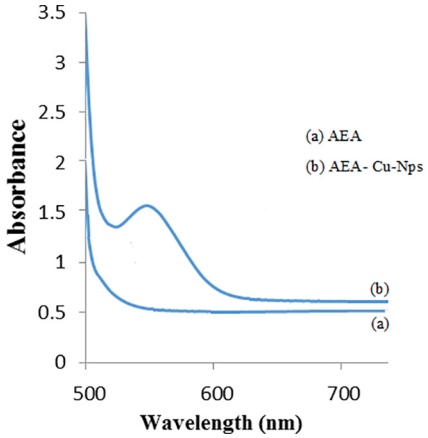

Fig. 2. UV–vis spectra of AEEA- Cu(II)-NPs.

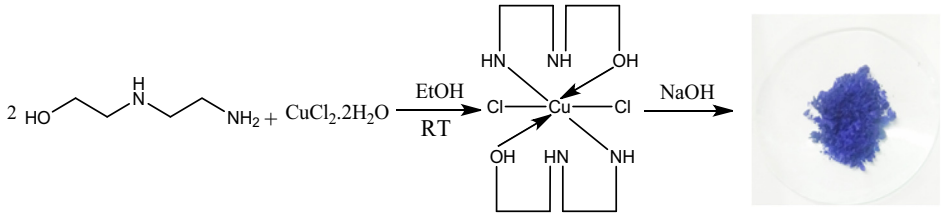

Scheme 1. Synthesis of Cu(II) nano catalysis (AEEA- Cu(II)-NPs).

allocated at 3299 cm^{-1} for **AEEA-Cu(II)-NPs**. The signal of 2942.21 cm^{-1} is C–H asymmetric stretching and 1022.05 cm^{-1}, and 1391 cm^{-1}, N–H bend only primary amine from 1591 cm^{-1} and N–H secondary amine change to primary amine due to the starch of Cu, which region obtained from 843 cm^{-1}, and also C–N stretch (aliphatic amines) for not connecting Cu region around 1242 cm^{-1} respectively.

3.1.4. Particle size analyzer studies

Particle size analyser technique was measured by analysis the particle size distribution and surface charge of the **AEEA-Cu(II)-NPs** NPs. Fig. 4 is indicated that first peak indicates that 70.7 nm of diameter and standard deviation 12.8, which indicates that 100 of average nano particles presence in the target nano catalysis. Fig. 4 shows that **AEEA-Cu(II)-NPs**, which indicated that particle size of 110 nm with a narrow index. Cu-Nps first peak intensity versus diameter is shown in Fig. 8 (Available in supporting information). Therefore, **AEEA-Cu(II)-NPs** is suitability for cancer targeting applications due to the nanoparticles was <100 nm.

3.1.5. SEM analysis

Fig. 3 shows the images of AEEA-Cu(II)-Nps in water (a) and in formamide (b). The **AEEA-Cu(II)-NPs** in water mixture shows 5 μm size, which is confirmed that nano participle formation of this combination.

3.1.6. Diffraction studies with X-rays

Investigation of phase crystalline and structural analysis was studied of **AEEA-Cu(II)-NPs**. The pattern of Cu nanoparticles is shown in Fig. 4 at 2θ values of 45.10°, 49.92°, and 73.10° respectively, showing that copper cubic lattice conformed to (111), (200), and (220) planes. JCPDS No. 040836 is indicating that good agreement and compared with centred cubic phase.

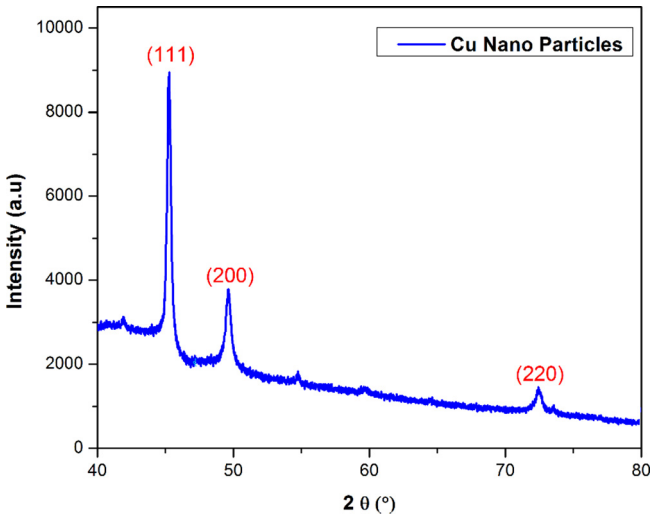

Fig. 4. XRD Studies of AEEA- Cu(II)-Nps mediated copper nanoparticle.

Table 1
Optimization the reaction type of catalyst.

S. No.	Catalysts	Yield (%)		
		0.5 Mole %	1 Mole %	2 Mole %
1	$TiCl_2$	–	–	–
2	$SnCl_2$	–	–	45
3	$ZnCl_2$	16	34	47
4	$ZrOCl_2$	–	–	14
5	$FeCl_2$	19	38	63
6	$CuCl_2$	26	68	
7	**Cu(Nps)**	**47**	**98**	

3.1.7. Synthesis and characterization of 2-thioxopyrimidine

Table 1 shows the optimization of catalyst for compound **1a**. The 2-thioxopyrimidine hydrazide derivatives were synthesized by using various catalysts such as, $TiCl_2$, $SnCl_2$, $ZnCl_2$, $ZrOCl_2$, $FeCl_2$, $CuCl_2$ and Cu(Nps) respectively. At the amount of catalyst load at 0.5, 1 Mole %, the catalysts $TiCl_2$, $SnCl_2$, $ZrOCl_2$ does not give the desired product. By using various metal chlorides as catalysts, $CuCl_2$ produces high yield of 68 % at 1 Mole %. Utilizing Cu (Nps) instead of $CuCl_2$ increases the yield from 68 % to 98 % at 1 Mole % respectively. Synthetic method of 2-thioxopyrimidine hydrazide was represented in Scheme 2. The mechanism of proposed compound was out lined in Scheme 3. In the proposed mechanism, initially the amine and ethylacetoacetate reacts to form 3-oxobutanehydrazide (I). Then the aldehyde and thiourea reacts to form benzylidenethiourea (II). The 3-oxobutanehydrazide (I) and benzylidenethiourea (II) combines to form an intermediate. Finally, the cyclization reaction occurs with the loss of water molecule and the elimination of catalyst to form the desired product. Analysis of the synthesized compound by FTIR, ^1H NMR, and ^{13}C NMR was performed. Compound **1a** displays the following absorption bands in its IR spectrum: 1100, 1625, 2724, 3179, and 3358 cm^{-1}, which corresponds to the functional groups of –C═S, Ph-Str, Ar-H, –NH, and –CONH, respectively. The ^1H NMR spectra shows that compound **1a** of sharp singlet at δ9.10 for NH proton, δ9.7 for NH_2,

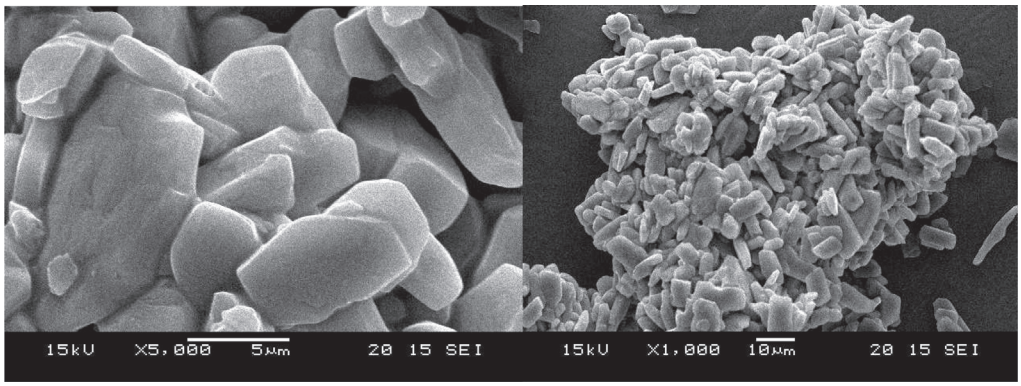

Fig. 3. AEEA-Cu(II)-Nps of SEM images.

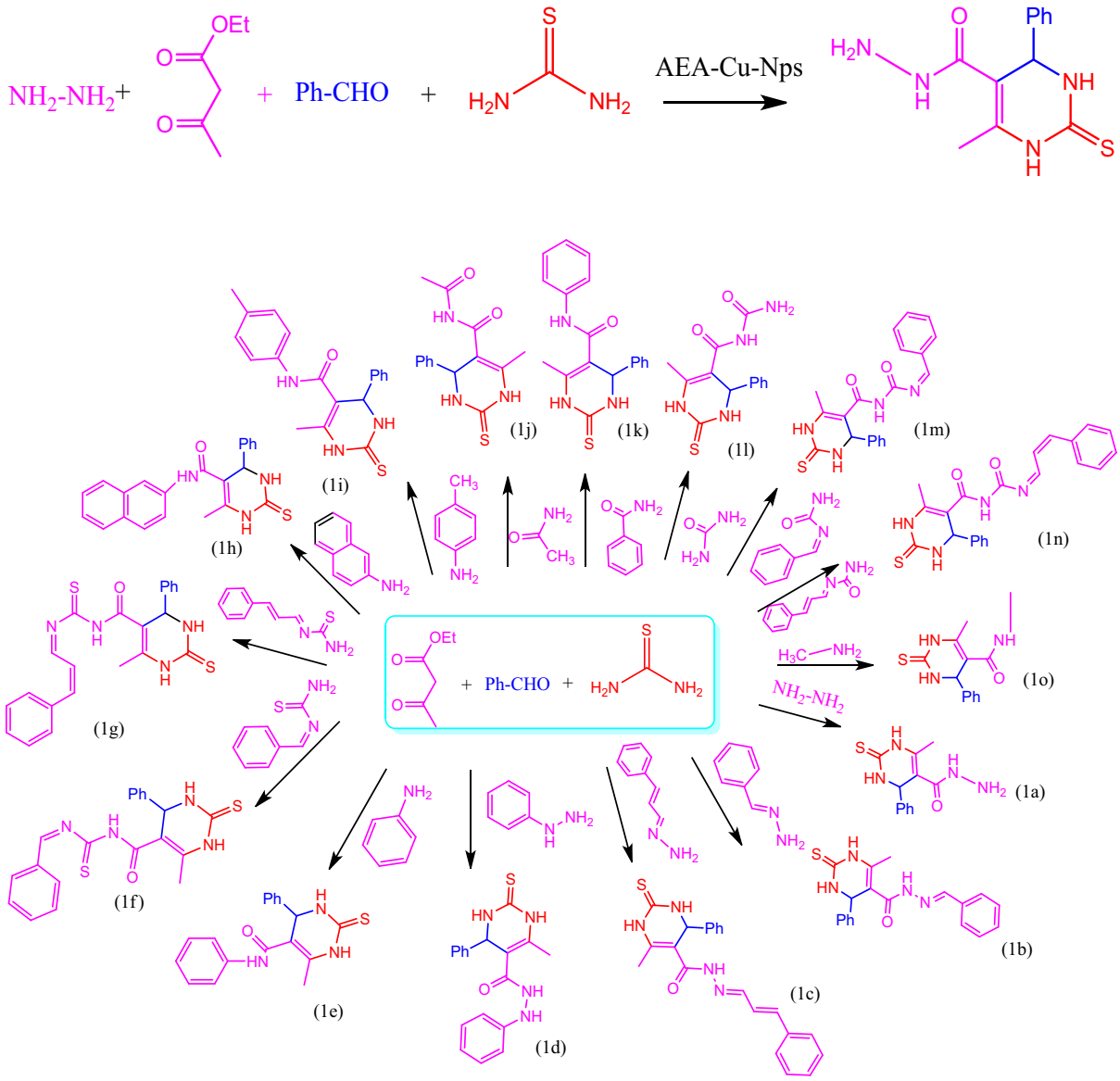

Scheme 2. Synthesis route of 2-thioxopyrimidine 5-carboxamide derivatives (1a-1o).

δ9.5 for –CONH, and δ 4.20 for –CH- proton respectably. The ^{13}C NMR peaks of C═S, CONH, and CH carbons are respectively at δ 174.0, δ 164.8, and δ 54.0 ppm.

3.1.8. Molecular geometry of compound 1a

Fig. 9 (See Supporting Info) shows the possible conformer of **1a** molecule enhanced at B3LYP level at 6-311G (d,p) level. The total energy of the conformer was determined to be −1158.09 a.u. for based on B3LYP/6–311 G (d,p) theory level. According to C1 point group symmetry, the title compound has the stablest conformer. Fig. 10 (See Supporting Info) shows the optimized molecular structure of compound **1a**. The pyrimidine ring at C1 and C6 is attached to carboxylic hydrazide and phenyl groups. Based on B3LYP/6-311G (d,p) levels, Table 2 (See Supporting Info) predicts the optimal bond lengths, angles, and dihedral angles for the molecule. Here are the optimizations for bond angles and bond lengths calculated with B3LYP, 6-311G(d,p). The bond distance between C-1 and C-2 according to B3LYP/6-311G(d,p) is 1.358 Å. A bond's longer length is a representation of the repellent and attractive forces of unlike charges. Calculated maximum bond length are C2 –C11 (1.504 Å), C6-C13 (1.528 Å) and C16-C17 (1.398 Å). Carbonyl group has a bond distance of 1.258 Å (O9-C7). Using B3LYP method, the optimal bond angle for C2-C1-C6 is 31.8o. The C1-C7-O9, C1-C7-N8 bonds have different angles (122.7o and 119.8o) and this is due to oxygen having a higher electron density than carbon and nitrogen, in other cases the hydrazide group will extend. In the molecule, C–C-H bonds increase and decrease in angles as they approach 120^0 degrees. The maximum bond angle for C–C–C bonds ends with a hydrogen atom in the molecule (C1-C2-C11: 127.2°, C6-C13-C18: 121.2°, C13-C14-C15: 120.6° and C16-C17-C18: 120.2°). The dihedral angle values of the molecule from 0° to 180° confirm its planarity.

3.1.9. Vibrational assignments

According to Table 3 (See Supporting Info), vibrational spectral assignments were achieved using the density functional theory (DFT) B3LYP/6-311G(d,p) based on theoretically predicted wavenumbers on recorded FT-IR spectra. The optimized geometry appears to be located the lowest energy point of the potential energy surface, as none of the predicted vibrational spectra have imaginary wavenumbers. DFT potentials systematically underestimate vibrational wavenumbers. It is possible to correct a signal

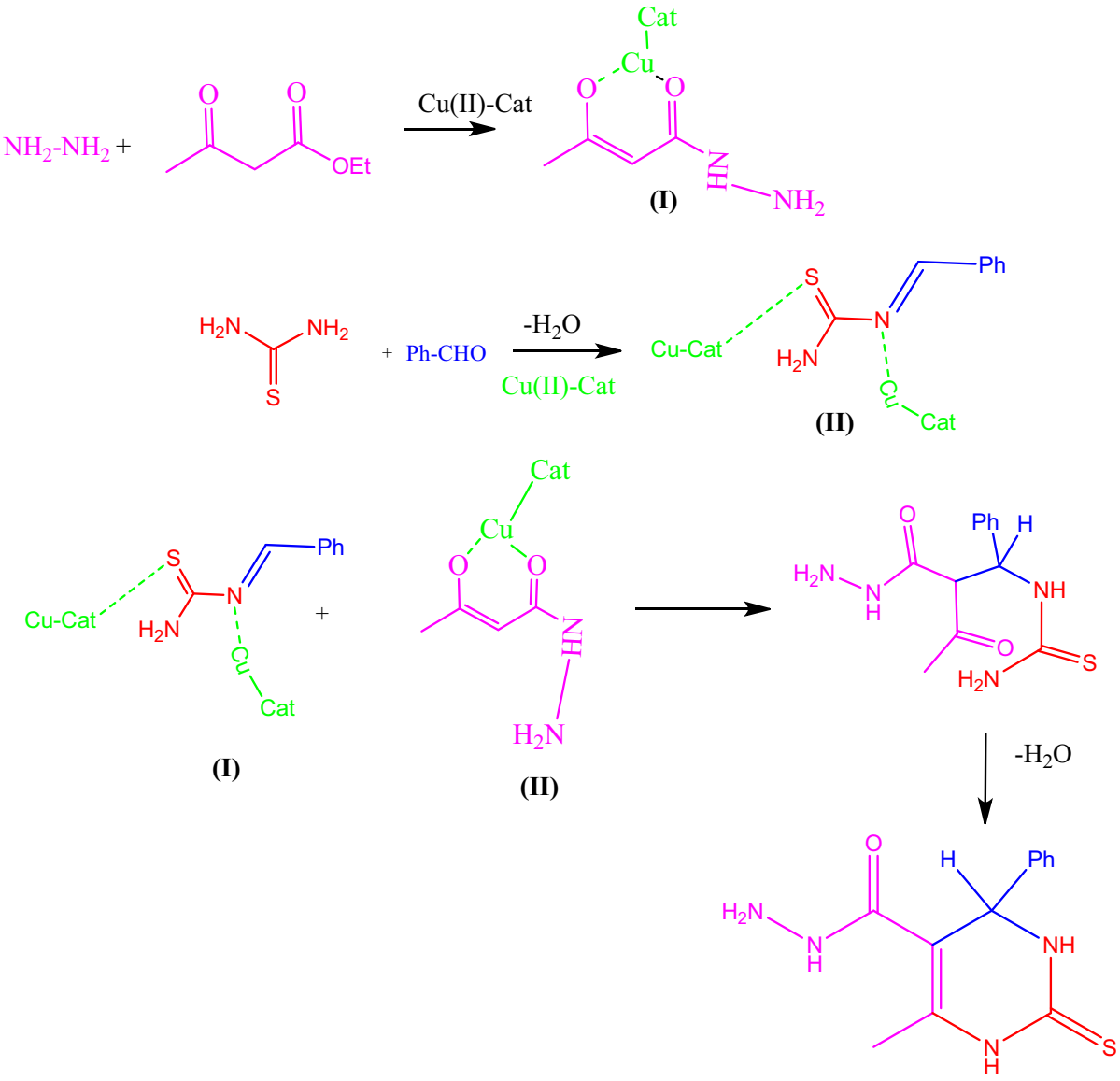

Scheme 3. Mechanism of formation of 2-thioxo pyrimidinehydrazide compound **1a**.

either by using anharmonic corrections explicitly, or directly scaling the wavenumbers. B3LYP was used to calibrate vibrational wavenumbers with scaling factors of 0.9663. Calibration values differ from experimental values by an average of <10 cm^{-1}. As a result of the electron correlation for this method, the wavenumbers calculated and experimental values show good agreement. Fig. 11 displays the calculated and experimental IR spectra of compound **1a**. (See Supporting Info for N–H, C–H, C=O, CH_3, and ring vibrations).

3.1.10. NMR analysis

Compound **1a** was optimized in terms of its molecular structure. The chemical shift calculations of molecule **1a** using ^{13}C NMR, gauge-including atomic orbital (GIAO), and ^{1}H NMR were conducted using B3LYP and 6-311G (d,p) basis sets. Gaussian 03 was used to calculate NMR spectra. According to chemical shifts, gas phase, calculations were executed in DMSO solution using the IEF-PCM model. Table 4 (See Supporting Info) shows that experimental and calculated ^{13}C and ^{1}H NMR values are well correlated. ^{1}H NMR (300 MHz, DMSO- d_6): δ 9.40 (s, 1H, CONH), 9.20 (s, 2H, NH), 7.19(t, 2H, Ph), 6.20 (2H, d, Ph), 5.48 (t, 1H, Ph), 4.20 (s, 1H, C-4), 2.2 (s, 2H,NH_2), 1.20 (s, 3H, CH_3); ^{13}C NMR (300 MHz): 174.2 (C=S), 165.0 (C=O), 158.0 (-6C-H), 143.0, 127.1, 128.3, 126.5 (6C, Ar ring), 100.0 (1C, 5C-H), 54.0 (1C, 4C-H), 14.0 (1C, $-CH_3$). Figure 12 and Figure 13 shows the calculated and experimental methods of ^{13}C NMR and ^{1}H NMR of compound **1a** (See Supporting Info).

3.1.11. GC-EI-MS analysis

In this study, the GC-EI-MS data support the significance of the proposed pyrimidine-5-carboxamide and observed for MS data. Molecular ionization is a well-established method leading to extensive fragmentation. For instance, radical-directed cleavage can produce the pyrimidine-5-carboxamide ion at *m*/*z* 262.33. Fragmentation of the upper ion spectra occurs by charge-directed mechanisms rather than by charge-remote means. A schematic illustration of EI-MS fragments for the analysis is shown in Scheme 4. Major structural fragments are embedded in this diagram. This spectrum is defined by the base peak of 42.08 *m*/*z* prop-1-ene ion. However, the pyrimidine-5-carboxamide does shift the (6-methyl-4-phenyl-2-thioxo-1,2,3,4-tetrahydropyrimidin-5-yl)(oxo)methylium and 6-methyl-4-phenyl-3,4-dihydropyr

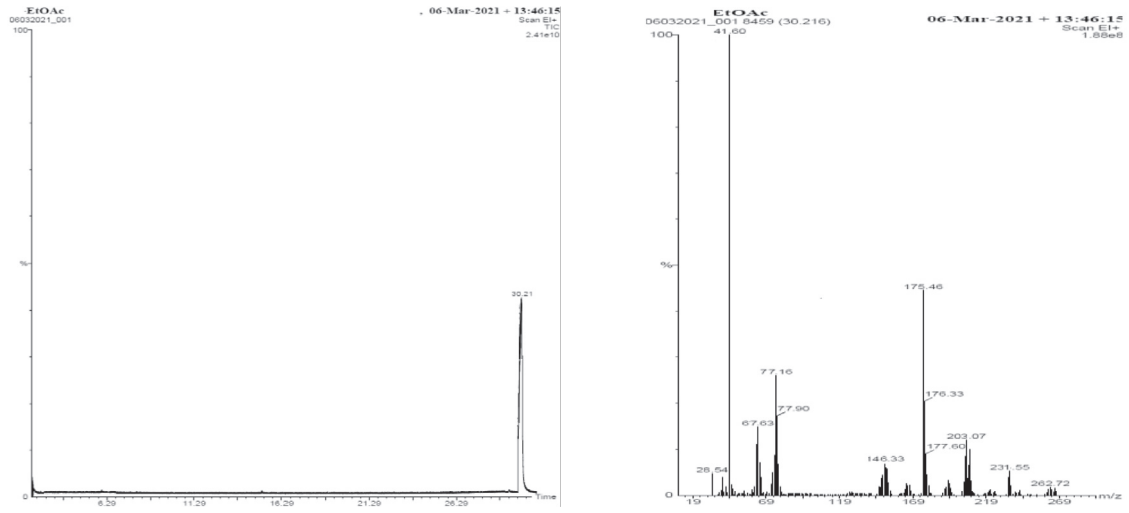

GC-EI-MS Perkin Elmer model GC clarus 680 and MS SQ8T (EI) for compound 1a

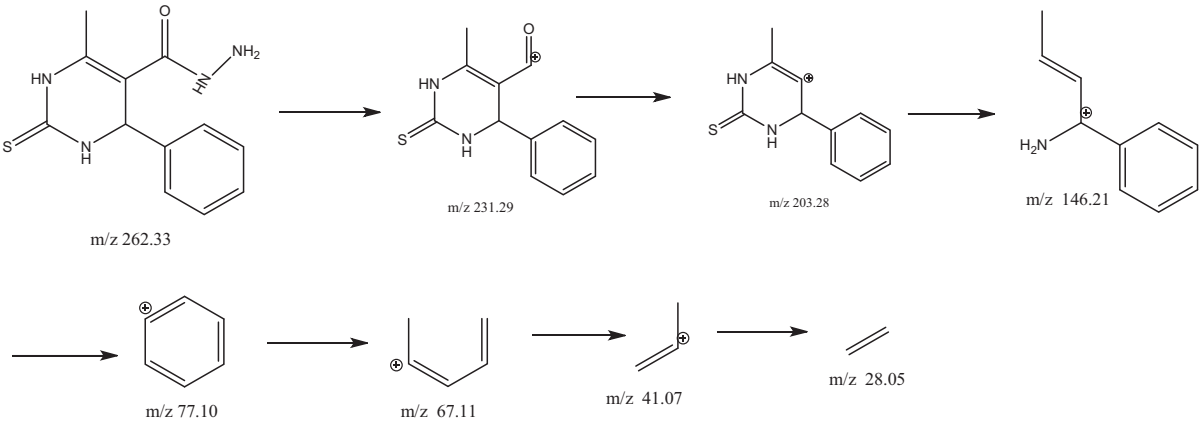

Scheme 4. Fragmentation pathways of compound 1a.

imi dine-2(1*H*)-thione ions by experimental peaks at *m*/*z* 231 and *m*/*z* 240, respectively. Prop-1-ene at *m*/*z* 154 is the base peak of this spectrum, which has no carbonyl carbon-^{13}C, as expected. Other peaks are obtained such as *m*/*z* 147.22, 132.20, 118.18, 78.11, 68.12, 42.08 and 28.05 respectively. In this study, same fragmentation pathways were observed for pyrimidine-5-carboxamide, when different substitutions were applied during synthesis.

3.1.12. HOMO–LUMO analysis

It is very important in quantum chemistry to know the lowest unoccupied molecular orbital (LUMO) and the highest occupied molecular orbital (HOMO). The atomic composition of the frontier molecular orbital is shown in Fig. 14 (See Supporting Info).

3.1.13. Molecular electrostatic potential (MEP)

A molecular electrostatic potential is a measure of electron density and is useful for describing electrophilic and nucleophilic sites, as well as interactions involving hydrogen bonds. As a result, examining electrostatic potentials V(r) can be an ideal way to model processes involving between the molecules, such as in drug-receptor interactions and enzyme-substance interactions, since two species sense each other through their electrostatic potentials. Calculations of the reactive MEP were made at optimized geometry (d, p) in B3LYP/6-311G, the molecular structure can be attacked by electrophilic and nucleophilic attacks. MEP positive (blue) and negative (red and yellow) regions were connected to electrophilicity and nucleophilicity, respectively, (Fig. 15, See Supporting Info). Oxygen atoms have negative regions, and hydrogen atoms have positive regions. In these results, we gain information regarding the region of the compound where intermolecular interaction and metallic bonding are possible. As a consequence, Fig. 11 (See Supporting Info) shows that there are no intermolecular interactions within the molecule.

3.1.14. Cytotoxic activity

To evaluate the cytotoxic potency of compounds (**1a-1o**), liver, cervical, and breast cancer cell lines were used. GI_{50}, TGI, and LC_{50} values were obtained for each derivative, and the results are expressed as GI_{50} growth inhibitor concentrations. The compounds **1f** and **1g** showed the highest level of activity against HepG2 (GI_{50} = 5.4 and 6.3 μm). In comparison with other compounds and fluorouracil, compounds **1f** and **1g** exhibited moderate activity against MCF-7 cancer cell lines, with GI_{50} values of 13.5 and 5.2 μm, respectively.

Fluorouracil is a pyrimidine counterpart that is used to diagnose a range of solid cancers such as colon, rectal, breast, gastric, pancreatic, ovarian, bladder, and liver cancer. Fluoruracil is transformed in vivo to the active metabolite 5-fluoroxyuridine monophosphate (F-UMP), keep in mind that we use fluorouracil as a standard of this study. These compounds had a moderate effect against HepG2 cancer cells in comparison to standard

Table 2
Cytotoxic activity of compounds (1a-1o).

Compounds	HepG2			MCF-7			HeLa		
	GI_{50} (μM)	TGI (μM)	LC_{50} (μM)	GI_{50} (μM)	TGI (μM)	LC_{50} (μM)	GI_{50} (μM)	TGI (μM)	LC_{50} (μM)
1a	15.6	32.3	>100	24.7	49.4	>100	23.4	46.9	86.3
1b	21.6	43.2	81.0	17.1	38.2	>100	43.8	86.3	>100
1c	17.9	48.2	88.2	7.8	15.2	54.6	21.3	43.6	89.3
1d	30.1	60.2	>100	21.0	43.1	86.4	23.2	46.9	91.2
1e	34.2	60.1	>100	20.1	42.4	86.3	38.2	66.2	>100
1f	5.4	12.5	62.5	13.5	26.9	83.5	16.8	34.7	92.8
1g	6.3	15.3	51.2	5.2	20.1	>100	8.1	17.1	65.3
1h	31.7	62.1	>100	22.6	52.5	88.4	29.8	52.6	>100
1i	37.9	57.9	92.9	40.7	67.9	>100	19.7	43.2	86.9
1j	34.8	65.8	>100	46.2	66.4	>100	43.8	72.4	>100
1k	51.0	72.1	91.8	34.9	64.9	95.7	51.7	78.9	>100
1l	61.6	84.8	>100	41.6	65.0	93.8	42.8	61.0	93.5
1m	18.6	30.3	81.9	21.7	44.8	64.9	27.9	41.0	86.9
1n	47.9	64.8	>100	41.8	63.8	>100	42.8	64.9	>100
1o	45.9	61.9	>100	27.6	58.9	>100	38.9	61.9	>100
Fluorouracil	43.2	62.3	>100	2.5	12.9	45.0	0.3	3.6	11.5

fluorouracil, but a lower effect in contradiction of MCF-7 and HeLa cancer cells. The cytotoxic results were summarized in Table 2.

3.1.15. Structure–activity relationship (SAR)

SAR can be used to assess a molecule's involvement in biological activity based on its chemical structure. It is necessary to use this process in order to identify the chemical groups/atoms responsible for modulating the bioactivity of a compound. In Fig. 5 shows that lipophilic domain part and electron donors groups of –C═S and –C═O, and the hydrogen bond domain of NH group, while the pyrimidine group provides biological activity. The following points were noted while conducting the SAR studies:

(i) A hydrazine group attached to pyrimidine makes compound **1a** more active than MCF-7 and HeLa cell lines.
(ii) As compared to fluorouracil, compound **1b** contained only a significant effect on HepG2 cancer cells, but it had no effect on any other cell lines tested.
(iii) Comparatively with **fluorouracil, 1c** containing allylidene-hydrazine on the pyrimidine showed inferior activity against the Hela and MCF-7 cancer cells as well as significant activity against the HepG2 cancer cells.
(iv) In comparison with **fluorouracil, 1d**, which contains the phenylhydrazine group attached to the pyrimidine, showed significant activity of HepG2 then very low activity against MCF-7 and HeLa cell lines.
(v) The cytotoxicity activity of **1e**, which consists of pyrimidine groups attached to an aniline group, was significant when compared with fluorouracil against HepG2 and only moderate against MCF-7 and HeLa cancer cells.
(vi) The compound **1f** containing benzylidenethiourea group was remarkably potent against HepG2 with GI_{50} values of 5.4 μm, whereas low activity against the other cell lines then fluorouracil. Fluorouracil has a diamide moiety that is similar to that in **1f**.
(vii) Compound **1g**, which consists of an allylidene thiourea group attached to the pyrimidine, responded well in contradiction of the HepG2 cell line (GI_{50} = 6.3 μm
(viii) Compound **1h**, which contains an attached naphthylamine group, displays superior activity against HepG2. However, it has poorer activity in contradiction of MCF-7 and HeLa cells.
(ix) The compound **1i**, which contains a p-methylaniline group devoted to the pyrimidine, exhibited significant activity against HepG2, but weak activity in contradiction of MCF-7 and HeLa cancer cells.

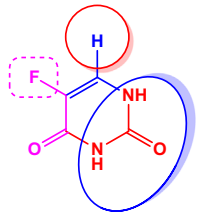

Fluorouracil
GI_{50}=43.2 μM against HepG2

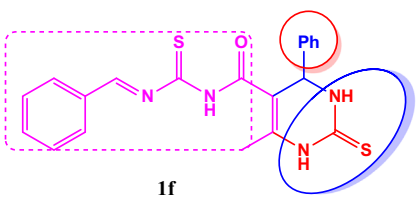

1f
GI_{50}=5.4 μM against HepG2

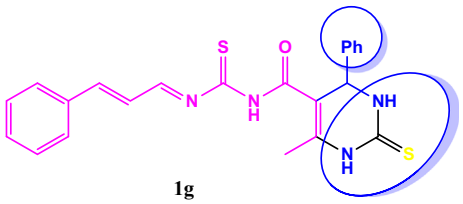

1g
GI_{50}=6.3 μM against HepG2

Fig. 5. Structure activity relationship.

(x) Compared to fluorouracil, compound **1j**, which has an acetamide group attached to the pyrimidine, displayed some activity in HepG2 cells, whereas less active for MCF-7 and HeLa cancer cell lines.
(xi) Compound **1k** is less energetic than fluorouracil against all types of cancer cell lines because it contains benzamide groups.
(xii) Compound **1l**, which contains urea groups attached to the pyrimidine, had a lower anticancer potency than fluorouracil.
(xiii) When compared to **fluorouracil,** compound **1m** containing benzylideneurea groups attached to the In HepG2 cells, pyrimidine demonstrated significant activity, but was not as effective in MCF-7 and HeLa cancer cells.
(xiv) Compound **1n** containing an allylideneurea group attached to the pyrimidine exhibited a lower level of activity by comparison with fluorouracil.
(xv) Fluorouracil was more effective against cancer cell lines than compound **1o**, which

Biological activity was determined by the position of the unsaturated thiourea moiety on the pyrimidine substituent in these preliminary SAR studies.

3.1.16. Molecular docking

In order to study the docking behavior between compounds **1f, 1g,** and the control **fluorouracil** with protein 4FM9, the Autodock Vina program was utilized (See Supporting Info for full details). As shown in Fig. 6, Fig. 16 (See Supporting Info), and 17 (See Supporting Info), these residues of the 4FM9 protein interact hydrophobically with compounds **1f, 1g**, and **fluorouracil** through hydrogen bonds and hydrophobic interactions. As shown in Table 3, the results are summarized.

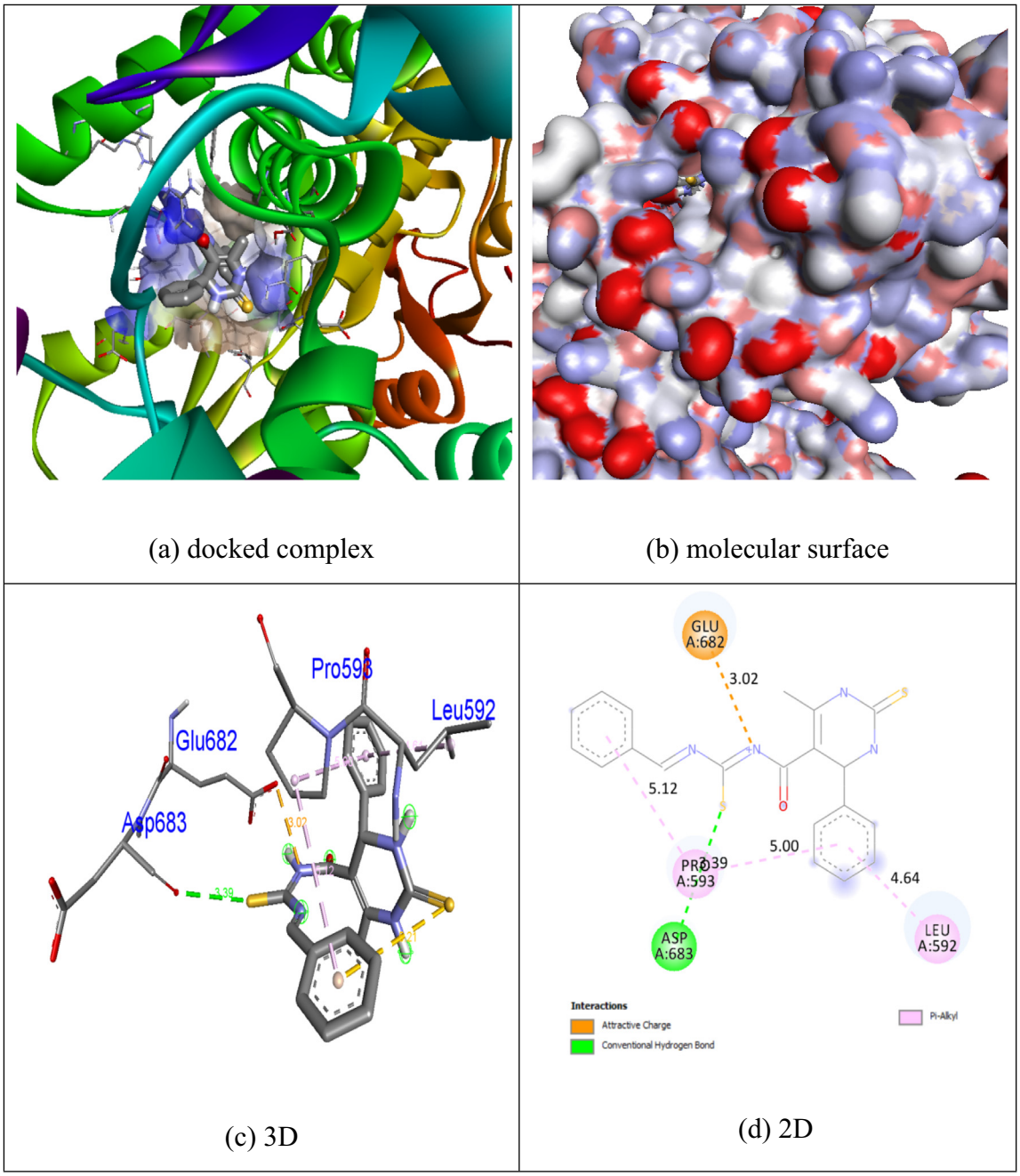

Fig. 6. Docking of compound 1f with binding pocket 4FM9.

Table 3
The cytotoxic protein 4FM9 is bound by compounds 1f, 1 g and fluorouracil in a docking study.

Proteins	Compound No.	Binding affinity (kcal/mol)	No. of H-bonds	H-bonding residues
4FM9	**1f**	−6.5	1	Asp683
	1g	6.1	2	Leu592, Glu702
	Fluorouracil	−5.4	3	Gln542, Tyr590, Leu685

Table 4
Analyses of the ADME and molecular properties of compounds 1f, 1g, and fluorouracil.

Comp.	tPSA (Topological polar surface area)	%Abs (Absorption)	MW (Molecular weight)	RoB (Number of rotatable bonds)	HBD (Number of hydrogen bond donors)	HBA (Number of hydrogen bonds acceptors)	MR (Molar refractivity)	IlogP (MlogP) (MlogP) (Logarithm of compound partition coefficient between n-octanol and water)	LogS (Logarithm of water solubility)	CYP2D6 Inhibitor
Rule	≤140 Å^2	>50	≤500	≤10	≤5	≤10	40–130	<5	>−4	–
1f	129.70	64.25	394.51	6	3	2	122.66	2.98 (2.15)	−4.20	No
1g	129.70	64.25	420.55	7	3	2	132.59	3.14 (2.52)	−4.55	No
Fluorouracil	65.72	86.32	130.08	0	2	3	27.64	0.44 (−0.32)	−0.58	No

3.1.17. Molecular property prediction and ADME

In the development of therapeutic agents, bioactive compounds play a major role (Newby et al., 2015) (See Supporting Info for full details). As shown in Table 4, the results are summarized.

4. Conclusion

A copper nanoparticle (**AEEA-Cu(II)-NPs**) was used to synthesize novel bioactive 2-thioxo-pyrimidine-5-carboxamides (**1a-1o**) and evaluated the cytotoxicity of cancer cell lines (HepG2, MCF-7, and HeLa). The compounds **1f** and **1g** were extremely effective against HepG2 cells compared to fluorouracil. During docking studies, **1f** showed a higher attraction for the 4FM9 protein (−6.5 kcal/mol) than **fluorouracil** (−5.4 kcal/mol). The compounds **1f**, and **1g** showed impressive inhibitory properties in cytotoxic screening as compared to the reference compound. DFT (B3LYP) analyses of vibrational and molecular structures have been conducted using a quantum mechanical approach. The vibrational spectra of compound **1a** was reported theoretically and experimentally. Calculations of the band gap energy have been done as well as visualizing the HOMO and LUMO orbitals. We calculated the ^{13}C NMR and ^{1}H NMR chemical shifts of compound **1a** using the B3LYP functional and the 6-311G (d,p) basis set, and the calculated results were in good agreement with the experimental ^{13}C NMR, and ^{1}H NMR. The DFT methods were also used to calculate molecular electrostatic potentials, as well as to identify the reactive sites. The GC-EI-MS technique is used to analyze fragmentation, which supports the synthesis of substituted pyrimidine-5-carboxamide derivatives. However, knowledge of systematic patterns for the above methods can support the identification of emerging synthetic drugs.

Declaration of Competing Interest

The authors declare that they have no known competing financial interests or personal relationships that could have appeared to influence the work reported in this paper.

Acknowledgment

This research work was funded by Researchers Supporting Project number (RSP-2021/27), King Saud University, Riyadh, Saudi Arabia.

Appendix A. Supplementary data

Supplementary data to this article can be found online at https://doi.org/10.1016/j.jksus.2022.101872.

References

Abu-Hashem, A.A., Youssef, M.M., Hussein, H.A.R., 2011. Synthesis, antioxidant, antituomer activities of some new thiazolo pyrimidines, pyrrolothiazolopyrimidines and triazolopyrrolothiazolopyrimidines derivatives. J. Chin. Chem. Soc. 58 (1), 41–48. https://doi.org/10.1002/jccs.201190056.

Agarwal, O.P., 2006. Organic Chemistry. Krishna Prakashan Media (P) Ltd, Reaction and Reagent. New Delhi, p. 735.

Alam, O., Khan, S.A., Siddiqui, N., Ahsan, W., Verma, S.P., Gilani, S.J., 2010. Antihypertensive activity of newer 1,4-dihydro-5-pyrimidine carboxamides: synthesis and pharmacological evaluation. Eur. J. Med. Chem. 45 (11), 5113–5119. https://doi.org/10.1016/j.ejmech.2010.08.022.

Atwal, K.S., O'Reilly, B.C., Gougoutas, J.A., Malley, M.F., 1987. Synthesis of Substituted 1,2,3,4-Tetrahydro-6-methyl-2-thioxo-5-pyrimidinecarboxylic Acid Esters. Heterocycles 26, 1189–1192. https://doi.org/10.3987/R-1987-05-1189.

Basavaraja, H.S., Sreenivasa, G.M., Jayachandran, E., 2005. Synthesis and biological activity of novel pyrimidinoimidazolines. Indian. J. Heterocycl. Chem. 15, 69.

Chiang, A.N., Valderramos, J.-C., Balachandran, R., Chovatiya, R.J., Mead, B.P., Schneider, C., Bell, S.L., Klein, M.G., Huryn, D.M., Chen, X.S., Day, B.W., Fidock, D.A., Wipf, P., Brodsky, J.L., 2009. Select pyrimidinones inhibit the propagation of the malarial parasite, Plasmodium falciparum. Bioorg. Med. Chem. 17 (4), 1527–1533. https://doi.org/10.1016/j.bmc.2009.01.024.

Daina, A., Zoete, V., 2016. A boiled-egg to Predict Gastrointestinal Absorption and Brain Penetration of Small Molecules. Chem. Med. Chem. 11, 1117-1121. https://dx.doi.org/10.1002%2Fcmdc.201600182.

Dewan, M., Kumar, A., Saxena, A., De, A., Mozumdar, S., Marr, A.C., 2012. Biginelli reaction catalyzed by copper nanoparticles. PLoS One 7 (8), e43078. https://doi.org/10.1371/journal.pone.0043078.

Ertl, P., Rohde, B., Selzer, P., 2000. Fast calculation of molecular polar surface area as a sum of fragment-based contributions and its application to the prediction of drug transport properties. J. Med. Chem. 43, 3714-3717. https://doi.org/10.1021/jm000942e.

Gupta, A.K., Sanjay, H.P., Kayath, A., Singh, G., Sharma, K.C., 1994. Anticonvulsant activity of pyrimidine thiols. Indian. J. Pharmacol. 26, 227–228.
Holzol, S., Preuss, W., Mehlin, A., 2006. Use of substituted 2,4-bis (alkylamino) pyrimidines. U.S. Patent. 0188453 A1.
Huang, X., Su, J., Rao, A.U., Tang, H., Zhou, W., Zhu, X., Chen, X., Liu, Z., Huang, Y., Degrado, S., Xiao, D., Qin, J., Aslanian, R., McKittrick, B.A., Greenfeder, S., Heek, M.V., Chintala, M., Palani, A., 2012. SAR studies of C2 ethers of 2H-pyrano[2,3- d] pyrimidine- 2,4,7(1H,3*H*)-triones as nicotinic acid receptor (NAR) agonist. Bioorg. Med. Chem. Lett. 22 (2), 854–858. https://doi.org/10.1016/j.bmcl.2011.12.041.
Ismaili, L., Nadaradjane, A., Nicod, L., Guyon, C., Xicluna, A., Robert, J.-F., Refouvelet, B., 2008. Synthesis and antioxidant activity evaluation of new hexahydropyrimido[5,4-c]quinoline-2,5-diones and 2-thioxohexahydropyrimido[5,4- c]quinoline-5- ones obtained by Biginelli reaction in two steps. Eur. J. Med. Chem. 43 (6), 1270–1275. https://doi.org/10.1016/j.ejmech.2007.07.012.
Juby, P.F., Hudyma, T.W., Brown, M., Essery, J.M., Partyka, R.A., 1979. Antiallergy agents. 1. 1,6-dihydro-6-oxo-2-phenylpyrimidine-5-carboxylic acids and esters. J. Med. Chem. 22 (3), 263–269. https://doi.org/10.1021/jm00189a009.
Kumar, B., Kaur, B., Kaur, J., Parmar, A., Anand, R.D., Kumar, H., 2002. Thermal/microwave assisted synthesis of substituted tetrahydropyrimidines as potent calcium channel blockers. Indian J. Chem. B 41, 526–1530.
Kumar, A., Maurya, R.A., 2007. An efficient bakers' yeast catalyzed synthesis of 3,4-dihydropyrimidin-2-(1*H*)-ones. Tetrahedron Lett. 48 (26), 4569–4571. https://doi.org/10.1016/j.tetlet.2007.04.130.
Lagoja, I., 2005. Pyrimidine as constituent of natural biologically active compounds. Chem. Biodivers. 2 (1), 1–50. https://doi.org/10.1002/cbdv.200490173.
Lee, H., Kim, B., Ahn, J., Kang, S., Lee, J., Shin, J., Ahn, S., Lee, S., Yoon, S., 2005. Molecular design, synthesis, and hypoglycemic and hypolipidemic activities of novel pyrimidine derivatives having thiazolidinedione. Eur. J. Med. Chem. 40 (9), 862–874. https://doi.org/10.1016/j.ejmech.2005.03.019.
Lewis, R.W., Mabry, J., Polisar, J.G., Eagen, K.P., Ganem, B., Hess, G.P., 2010. Dihydropyrimidinone positive modulation of delta-subunit-containing gamma-aminobutyric acid type A receptors, including an epilepsy-linked mutant variant. Biochemistry. 4841-4851. https://dx.doi.org/10.1021%2Fbi100119t.
Mokale, S.N., Shinde, S.S., Elgire, R.D., Sangshetti, J.N., Shinde, D.B., 2010. Synthesis and anti- inflammatory activity of some 3-(4,6-disubtituted-2-thioxo-1,2,3,4-tetrahydropyrimidin- 5-yl) propanoic acid derivatives. Bioorg. Med. Chem. Lett. 20 (15), 4424–4426. https://doi.org/10.1016/j.bmcl.2010.06.058.
Newby, D., Freitas, A.A., Ghafourian, T., 2015. Decision trees to characterise the roles of permeability and solubility on the prediction of oral absorption. Eur. J. Med. Chem. 90, 751–765. https://doi.org/10.1016/j.ejmech.2014.12.006.
Nezu, Y., Miyazaki, M., Sugiyama, K., Kajiwara, I., 1996. Dimethoxypyrimidine as novel herbicides—part1: synthesis and herbicidal activity of dimethoxyphenoxypyrimidines and analogues. Pestic. Sci. 47, 103–113. https://doi.org/10.1002/(SICI)1096-9063(199606)47:2%3C103::AID-PS396%3E3.0.CO;2-Z.
Pasunooti, K.K., Chai, H., Jensen, C.N., Gorityala, B.K., Wang, S., Liu, X.-W., 2011. A microwave- assisted, copper-catalyzed three-component synthesis of dihydropyrimidinones under mild conditions. Tetrahedron Lett. 52 (1), 80–84. https://doi.org/10.1016/j.tetlet.2010.10.150.
Porter, A.E., 1979. Diazines and Benzodiazines. Pregamon Press, Elsevier Science BV Amsterdam, Netherlands, p. 14.
Rahaman, S.A., Rajendra Pasad, Y., Kumar, P., Kumar, B., 2009. Synthesis and anti-histaminic activity of some novel pyrimidines. Saudi Pharmaceut. J. 17 (3), 255–258. https://doi.org/10.1016/j.jsps.2009.08.001.
Ram, V.J., Haque, N., Guru, P.Y., 1992. Chemotherapeutic agents XXV: synthesis and leishmanicidal activity of carbazolylpyrimidines. Eur. J. Med. Chem. 27 (8), 851–855. https://doi.org/10.1016/0223-5234(92)90121-G.
Rana, K., Kaur, B., Kumar, B., 2004. Synthesis and anti-hypertensive activity of some dihydropyrimidines. Indian J. Chem. B 43, 1553–1557.
Rodrigues, A.L.S., Rosa, J.M., Gadotti, V.M., Goulart, E.C., Santos, M.M., Silva, A.V., Sehnem, B., Rosa, L.S., Gonçalves, R.M., Corrêa, R., Santos, A.R.S., 2005. Antidepressant-like and antinociceptive- like actions of 4-(4′-chlorophenyl)-6-(4″-methylphenyl)-2-hydrazinepyrimidine Mannich base in mice. Pharmacol. Biochem. Behav. 82 (1), 156–162. https://doi.org/10.1016/j.pbb.2005.08.003.
Sondhi, S.M., Jain, S., Dwivedi, A.D., Shukla, R., Raghubir, R., 2008. Synthesis of condensed pyrimidines and their evaluation for anti-inflammatory and analgesic activities. Indian J. Chem. B 47, 136–143.
Storer, R., Moussa, A., La Colla, P., Artico, M., 2005. Oxo-pyrimidine compounds. U.S. Patent, 0014774 A1.
Surendra Kumar, R, Idhayadhulla, A, Jamal Abdul Nasser, A, Murali, k, 2011. Synthesis and anticancer activity of some new series of 1, 4-dihydropyridine derivatives. Indian J. Chem. Sect. B. 50 (8), 1140–1144.
Surendra Kumar, R, Moydeen, M, Al-Deyab S, S, Manilal, A, Idhayadhulla, A, 2017. Synthesis of new morpholine-connected pyrazolidine derivatives and their antimicrobial, antioxidant, and cytotoxic activities. Bioorganic Med. Chem. Lett. 27 (1), 66–71. https://doi.org/10.1016/j.bmcl.2016.11.032.
Suresh, Sandhu, J.S., 2012. Past, present and future of the Biginelli reaction: a critical perspective. ARKIVOC (i) 2012 (1), 66–133. https://doi.org/10.3998/ark.5550190.0013.103.
Trivedi, A.R., Bhuva, V.R., Dholariya, B.H., Dodiya, D.K., Kataria, V.B., Shah, V.H., 2010. Novel dihydropyrimidines as a potential new class of antitubercular agents. Bioorg. Med. Chem. Lett. 20 (20), 6100–6102. https://doi.org/10.1016/j.bmcl.2010.08.046.
Vega, S., Alonso, J., Diaz, J.A., Junquera, F., 1990. Synthesis of 3-substituted-4-phenyl-2- thioxo- 1,2,3,4,5,6,7,8-octahydrobenzo[4,5]thieno[2,3-d]pyrimidines. J. Heterocycl. Chem. 27, 269–273. https://doi.org/10.1002/jhet.5570270229.
Wang, G.B., Wang, X., Lou, W., Hao, J., 2011. Gold-ionic liquid nanofluids with preferably tribological properties and thermal conductivity. Nanoscale Res. Lett. 6, 251–259. https://doi.org/10.1186/1556-276X-6-259.
Xie, F., Zhao, H., Zhao, L., Lou, L., Hu, Y., 2009. Synthesis and biological evaluation of novel 2,4,5-substituted pyrimidine derivatives for anticancer activity. Bioor. Med. Chem. Lett. 19 (1), 275–278. https://doi.org/10.1016/j.bmcl.2008.09.067.
Yarapathi, R.V., Kurva, S., Tammishetti, S., 2004. Synthesis of 3,4-dihydropyrimidin-2(1H)ones using reusable poly(4-vinylpyridine-co-divinylbenzene)-Cucomplex. Catal. Commun. 5, 511–513. https://doi.org/10.1016/j.catcom.2004.06.007.